

Flow of Casson Fluid Through Circular Porous Bearing

 Open
Access

 Sampath Kumar¹, Nithyanand Pai^{1,*}
¹ Manipal Institute of Technology, Manipal Academy of Higher Education, Manipal, India

ARTICLE INFO

Article history:

Received 20 May 2020

Received in revised form 19 July 2020

Accepted 24 July 2020

Available online 30 July 2020

ABSTRACT

The present work is connected with fluid dynamics aspects of circular slider. It is study about flow of Casson fluid through circular porous bearing. In this model Casson fluid is forced through the porous bottom of a circular slider which is moving laterally on a horizontal plane. The governing Navier Stokes equations are derived and reduced to nonlinear ordinary differential equations through transformations. The problem is analysed through Homotopy Perturbation Method (HPM) and Finite Difference Method (FDM). The effective terms in the HPM representing the physical parameters reveal the qualitative features of the flow. The results are presented for the velocity, wall gradients of vertical velocity functions and lateral velocity functions values in its absolute values with cross Reynolds number. The results are validated by two methods and are in good agreement. They show that they are increasing at one wall and decreasing at the other wall. It is clear that the efficiency of porous slider bearing increases in case of the Casson fluid. The model has application in hydrostatic thrust bearings and air cushioned vehicles. Further friction is greatly reduced in the present case. So it has importance in industry and technology.

Keywords:

Casson fluid; porous slider; Navier-Stokes equations; nonlinear differential equations; HPM; FDM

Copyright © 2020 PENERBIT AKADEMIABARU - All rights reserved

1. Introduction

The study about the porous slider bearing is vital in the field of research, as the application is used in the growth of industry and technology. Sliding friction is greatly reduced if a fluid is forced between two solid surfaces. The porous sliders are important in fluid cushioned moving pads (examples include hydrostatic thrust bearings and air cushioned vehicles). Many authors [1-3] contributed their efforts to understand these types of problems, firstly C Y Wang [4] in 1976 studied about the circular porous slider. In 1984 R. Subba reddy [5] analysed the flow and thermal characteristics of a circular porous slider for a Newtonian fluid for Reynolds number 0.01 to 50. In 1993 N. M. Bujurke [6] and his associates studied the circular porous slider through computer extended series. Recent developments about slider bearing can be obtained from the articles [7,8].

* Corresponding author.

E-mail address: nppaimit@yahoo.co.in (Nithyanand Pai)

<https://doi.org/10.37934/cfdl.12.7.4856>

Method of solution is also plays an important role for these kind of problems, many authors used the numerical technique to solve the problem in the past. Solving these type of problems using semi-numerical method is an alternative technique. Homotopy perturbation method first proposed by Ji-Huan He [9] in 1998. HPM is the combination of traditional perturbation method and homotopy in topology. In 2013 Sumit gupta [10] and his associates applied this method for solving nonlinear wave-like equations. This method is useful for solving the different class of problems in the applied mathematics (like, functional integral equations [11], coupled system of reaction diffusion equation [12], Helmholtz equation and fifth-order Kdv equation [13], the epidemic model [14] etc.). Homotopy perturbation method for squeezing flow between parallel plates has been successfully used [15-19]. Recently, different kind of study about the fluid flow is done by Shaw and his associates [20,21].

The present work is concerned with the Non-Newtonian fluid flow through the circular porous slider bearing and presents the importance of Non-Newtonian fluid compared to Newtonian fluid. The governed Navier stokes equations are reduced to coupled non-linear differential equations. In the present paper we analysed the considered problem with HPM and compared the results with classical FDM. The main advantage of HPM is that it yields a very rapid convergence of the series solution, only with the few iterations. For simple domains the HPM has advantages over pure numerical results. A single computer program gives the solution for a large range of expansion quantity. Once the convergence is guaranteed the results can be obtained for the desired accuracy. Further the method reveals the analytic structure of the solution which is not found in numerical solutions.

2. Problem Formulation

This model is representing a flow between two plates T_1 and T_2 . Whereas one plate is solid (lower plate T_1) and the upper one is porous through which fluid is injected. An incompressible Casson fluid is forced through the porous wall of the slider with a velocity W as shown in Figure 1 below.

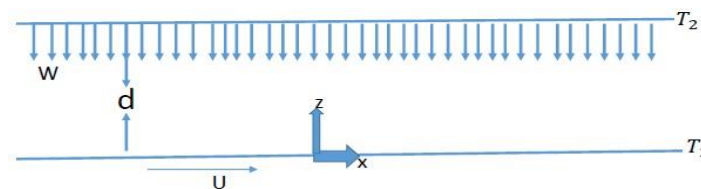


Fig. 1. Geometry of the problem

The ground is the plane $z = 0$ moving in the x direction with velocity u . Since the gap width d is small we may assume that both plane extended to infinity. The continuity and momentum equations for the problem is as follows

$$\frac{\partial u}{\partial x} + \frac{\partial v}{\partial y} + \frac{\partial w}{\partial z} = 0 \tag{1}$$

$$u \frac{\partial u}{\partial x} + v \frac{\partial u}{\partial y} + w \frac{\partial u}{\partial z} = -\frac{1}{\rho} \frac{\partial p}{\partial x} + \left(1 + \frac{1}{\gamma}\right) \left[\frac{\partial^2 u}{\partial x^2} + \frac{\partial^2 u}{\partial y^2} + \frac{\partial^2 u}{\partial z^2}\right] \tag{2}$$

$$u \frac{\partial v}{\partial x} + v \frac{\partial v}{\partial y} + w \frac{\partial v}{\partial z} = -\frac{1}{\rho} \frac{\partial p}{\partial y} + \left(1 + \frac{1}{\gamma}\right) \left[\frac{\partial^2 v}{\partial x^2} + \frac{\partial^2 v}{\partial y^2} + \frac{\partial^2 v}{\partial z^2}\right] \tag{3}$$

$$u \frac{\partial w}{\partial x} + v \frac{\partial w}{\partial y} + w \frac{\partial w}{\partial z} = -\frac{1}{\rho} \frac{\partial p}{\partial z} + \left(1 + \frac{1}{\gamma}\right) \left[\frac{\partial^2 w}{\partial x^2} + \frac{\partial^2 w}{\partial y^2} + \frac{\partial^2 w}{\partial z^2}\right] \tag{4}$$

The boundary conditions are

$$z = 0 \quad u = U, v = w = 0, T = T_1$$

$$z = d \quad u = v = 0, w = -W, T = T_2$$

By using the following transformation

$$\eta = \frac{z}{d}, u = Uf(\eta) + W\frac{x}{d}H'(\eta), v = \frac{W}{d}yH'(\eta), w = -2WH(\eta) \quad (5)$$

Substituting Eq. (5) in Eq. (2) to Eq. (4) one can get

$$\left(1 + \frac{1}{\gamma}\right)H'''' + 2RH'''' = 0 \quad (6)$$

$$\left(1 + \frac{1}{\gamma}\right)f'' + 2RHf' - R H'f = 0 \quad (7)$$

Subjected to the boundary conditions

$$H(0) = H'(0) = 0, f(0) = 1 \quad (8)$$

$$H(1) = \frac{1}{2}, H'(1) = 0, f(1) = 0$$

3. Method of Solution

We adopt two methods to solve the considered problems.

3.1 Homotopy Perturbation Solution (HPM)

To describe the HPM solution for the system of non-linear differential equations, we consider

$$D_1[H(\eta)] - f_1(\eta) = 0 \quad (9)$$

$$D_2[f(\eta)] - f_2(\eta) = 0 \quad (10)$$

where D_1 and D_2 denotes the operator, $H(\eta)$ and $f(\eta)$ are unknown functions, η denote the independent variable and f_1, f_2 are known functions. D_1 and D_2 can be written as

$$D_1 = L_1 + N_1$$

$$D_2 = L_2 + N_2$$

where L_1 and L_2 are simple linear part, N_1 and N_2 are remaining part of the Eq. (9) and Eq. (10) respectively.

The proper selection of $L_1, L_2, N_1,$ and N_2 form the governing equations one can get the homotopy Eq. (9) and Eq. (10) as follows

$$H_1(\phi_1(\eta, q; q)) = (1 - q)[L_1(\phi_1, q) - L_1(v_0(\eta))] + q[D_1(\phi_1, q) - f_1(\eta)] = 0 \quad (11)$$

$$H_2(\phi_2(\eta, q; q)) = (1 - q)[L_2(\phi_2, q) - L_2(v_0(\eta))] + q[D_2(\phi_2, q) - f_2(\eta)] = 0 \quad (12)$$

where $v_0(\eta)$ is the initial guess to the Eq. (11) and Eq. (12). We assume the solution of Eq. (11) and Eq. (12). as follows,

$$\phi_1(\eta, q) = \sum_{n=0}^{\infty} q^n H_n(\eta) \quad (13)$$

$$\phi_2(\eta, q) = \sum_{n=0}^{\infty} q^n f_n(\eta) \quad (14)$$

The solution to the considered problem is Eq. (13) and Eq. (14) at $q = 1$. The zeroth and first order solutions for the considered problem are as follows

$$H_0(\eta) = 1.5\eta^2 - \eta^3$$

$$H_1(\eta) = \frac{R\gamma\eta^2 \left(\begin{array}{c} 0.09286 - 0.12857\eta + 0.05\eta^2 - 0.01429\eta^5 \\ + \gamma \left(\begin{array}{c} 0.185714 - 0.25714\eta + 0.1\eta^4 \\ - 0.02857\eta^5 \end{array} \right) \end{array} \right)}{(1+\gamma)^3} + \gamma^2(0.092857 - 0.12857\eta + 0.05\eta^4 - 0.01428\eta^5)$$

$$f_0 = 1 - \eta$$

$$f_1 = \frac{0.05R\gamma\eta(-6 + 10\eta^2 - 5\eta^3 + \eta^4)}{1 + \gamma}$$

3.2. Finite Difference Method (FDM)

The equations mentioned above Eq. (6), Eq. (7) and Eq. (8) were solved numerically by FDM to confirm the results obtained by us. Using standard finite difference method, i.e stepping from η_{j-1} to η_j , a Crank-Nicolson's scheme was used. These tridiagonal systems are easily solved to update the values on each grid point. Calculations were performed by dividing the interval into 10^4 sub intervals to find the associated parameters. These system of equations were solved using Mathematica.

4. Results and Discussion

In the present study, we consider the problem of circular porous slider bearing for Casson fluid. The problem is analysed through HPM for velocity distribution, wall gradients of velocity functions for the various values of cross flow Reynolds number with Casson parameter. In case of HPM, first we generate two terms manually, as algebra becomes cumbersome we use mathematica code systematically to get the terms up to order of $n = 15$. Further an efficient finite difference scheme is used to solve the same boundary value problem. In this discretization process an interval $[0, 1]$ is divided in to 10^4 subdivisions to get accurate results.

The HPM results for velocity distributions are shown in Figure 2, Figure 3 and Figure 4. We observed from Figure 2 that the vertical velocity $H(\eta)$ increases within the gap width as R increases. On increasing the non-Newtonian characteristic parameter (γ) the same nature observed from Figure

3 and Figure 4, however a small change one can observe from Figure 3 and Figure 4, it is due to the non-Newtonian characteristics of the fluid, as γ increases the fluid flow between plates acquire the characteristic of the non-Newtonian fluid. The fluid becomes thicker and the velocity of the fluid for various values of R becomes more distinguishable.

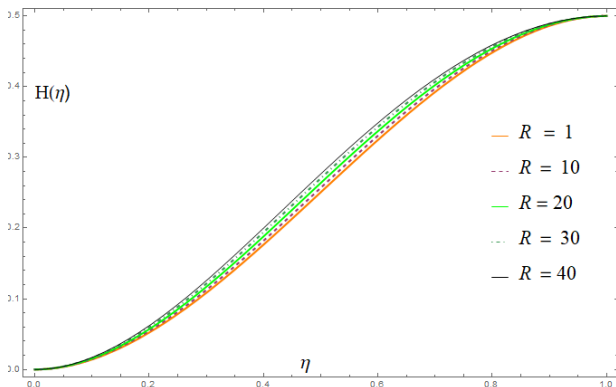


Fig. 2. Vertical velocity profile $H(\eta)$, $\gamma = 0.1$

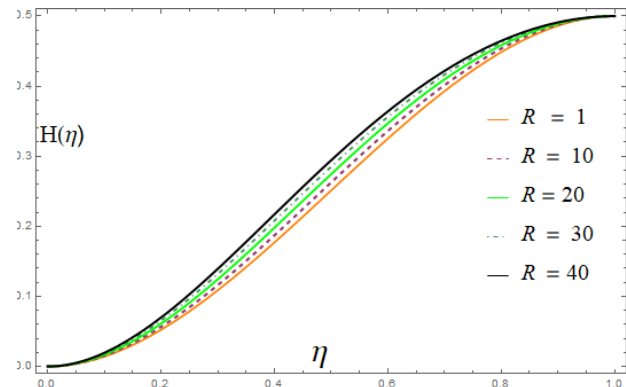


Fig. 3. Vertical velocity profile $H(\eta)$, $\gamma = 0.2$

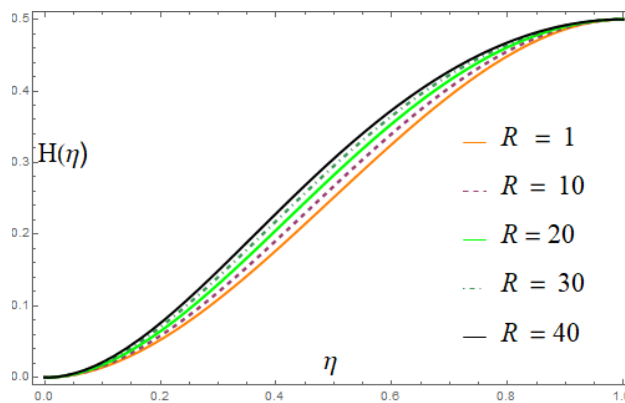


Fig. 4. Vertical velocity profile $H(\eta)$, $\gamma = 0.3$

Figure 5, Figure 6 and Figure 7 represents the lateral velocity profile $H'(\eta)$. From Figure 5 one can notice that the lateral velocity profile $H'(\eta)$ is parabolic for small values of R and becomes highly unsymmetrical as R increases. On increasing the cross-flow Reynolds numbers, the amplitude of $H'(\eta)$ increases whereas the position of maximum velocity tends to move closer to the moving wall. Figure 6 and Figure 7 also show the same pattern for different values of the γ . In a way from Figure 5, Figure 6 and Figure 7 it is notable that the vertical velocity $H'(\eta)$ increases in $0 \leq \eta \leq 0.5$ as R increases and decreases in $0.5 \leq \eta \leq 1$.

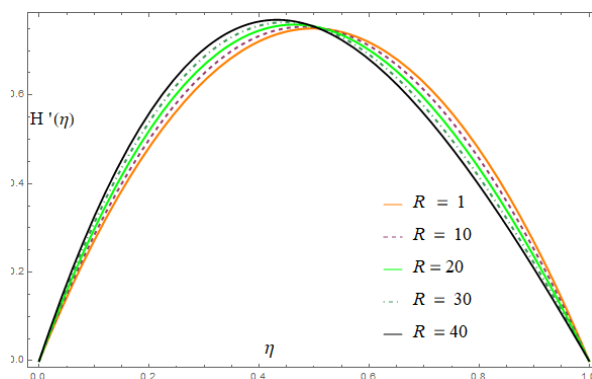


Fig. 5. Lateral velocity profile $H'(\eta)$, $\gamma = 0.1$

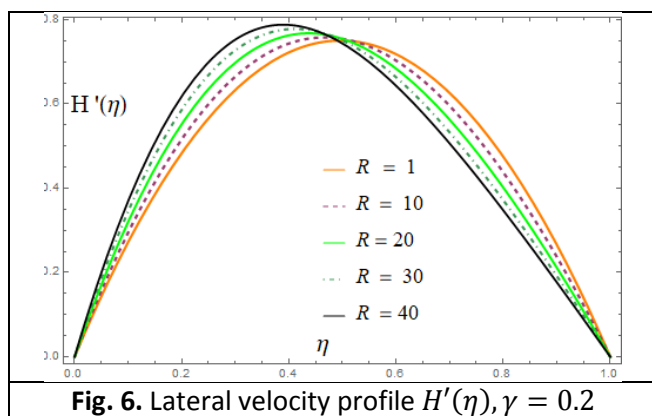


Fig. 6. Lateral velocity profile $H'(\eta)$, $\gamma = 0.2$

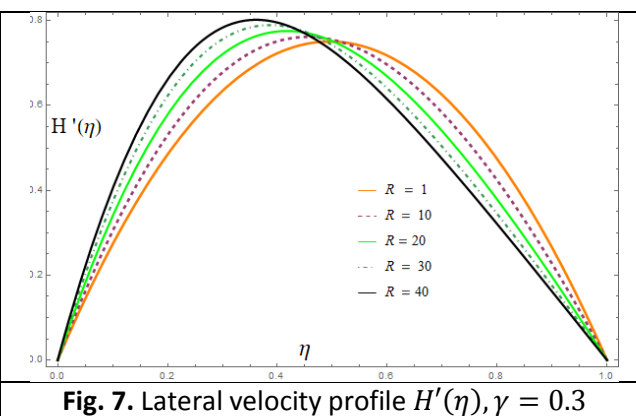


Fig. 7. Lateral velocity profile $H'(\eta)$, $\gamma = 0.3$

The semi-numerical results for lateral velocity $f(\eta)$ presented in Figures 8 to 10. In all these figures the lateral velocity is linear for the small values of the parameter R while it becomes highly non-linear for increasing the values of cross-flow Reynolds numbers. Other side one can observe that the value of $f(\eta)$ decreases as R increases. More importantly from these figures we observed that lateral velocity becomes highly non-linear for increasing the non-Newtonian characteristic of the fluid.

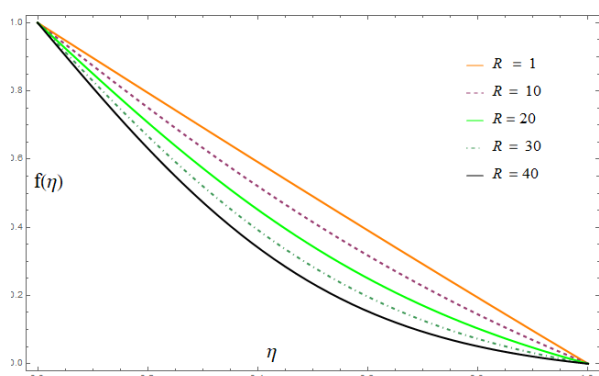


Fig. 8. Lateral velocity profile $f(\eta)$, $\gamma = 0.1$

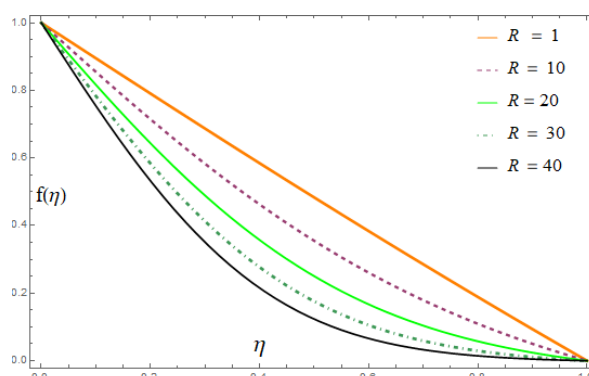


Fig. 9. Lateral velocity profile $f(\eta)$, $\gamma = 0.2$

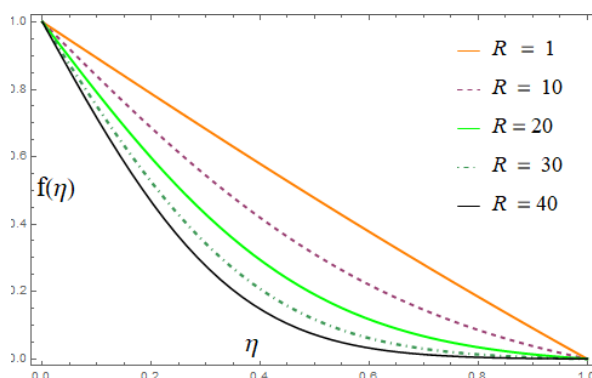


Fig. 10. Lateral velocity profile $f(\eta)$, $\gamma = 0.3$

Wall gradients of vertical velocity functions for various values of the cross flow Reynolds number are presented in Table 1, Table 2, Table 3 and Table 4. Wall gradients of lateral velocity functions for various values of the cross flow Reynolds number are presented in Table 5 and Table 6. Also, we compared the HPM solution with FDM to validate the results and observed that they are in good agreements. It is observed that the absolute values of wall gradients $H''(0)$, $H'''(0)$ and $f(0)$ are increasing with increase in R and γ values. But Table 2, Table 4 and Table 6 indicate the absolute

values of $H''(1)$, $H'''(1)$ and $f'(1)$ decrease as R and γ increase. This is due to non-Newtonian characteristics parameter and injection effect at the wall.

Table 1
 The values of $H''(0)$

R	γ	HPM	FDM	γ	HPM	FDM	γ	HPM	FDM
1	0.1	3.01691	3.01609	0.2	3.03106	3.03076	0.3	3.04306	3.04227
		3.08518	3.08518		3.15726	3.15684		3.21893	3.21850
		3.17178	3.17070		3.31874	3.31761		3.44508	3.44418
		3.25961	3.25874		3.48325	3.48278		3.67524	3.67460
		3.34846	3.34749		3.64956	3.64825		3.90635	3.90554
		3.43815	3.43733		3.81654	3.81573		4.13583	4.13514
		3.52848	3.52771		3.98314	3.98111		4.36165	4.36073
		3.61924	3.61922		4.14848	4.14702		4.58248	4.58156
		3.71026	3.70973		4.31186	4.31132		4.79767	4.79580

Table 2
 The values of $H''(1)$

R	γ	HPM	FDM	γ	HPM	FDM	γ	HPM	FDM
1	0.1	-2.97164	-2.97124	0.2	-2.94832	-2.94663	0.3	-2.92881	-2.92853
		-2.86231	-2.86044		-2.75529	-2.75459		-2.67004	-2.66914
		-2.73471	-2.73455		-2.54336	-2.54335		-2.40092	-2.40096
		-2.61680	-2.61627		-2.36144	-2.36047		-2.18482	-2.18403
		-2.50814	-2.50754		-2.20647	-2.20717		-2.01329	-2.01327
		-2.40825	-2.40799		-2.07524	-2.07454		-1.87802	-1.87767
		-2.31664	-2.31602		-1.96457	-1.96494		-1.77147	-1.77148
		-2.23279	-2.23169		-1.87141	-1.87184		-1.68729	-1.68661
		-2.15618	-2.15528		-1.79301	-1.79238		-1.62126	-1.61982

Table 3
 The values of $H'''(0)$

R	γ	HPM	FDM	γ	HPM	FDM	γ	HPM	FDM
1	0.1	-6.07039	-6.06860	0.2	-6.12946	-6.12949	0.3	-6.17972	-6.17841
		-6.35720	-6.35869		-6.66471	-6.66459		-6.93170	-6.93168
		-6.72727	-6.72462		-7.37135	-7.36812		-7.94138	-7.93168
		-7.10973	-7.10784		-8.11659	-8.11639		-9.01923	-9.01875
		-7.50409	-7.50174		-8.89645	-8.89306		-10.15380	-10.1527
		-7.90973	-7.90857		-9.70658	-9.70499		-11.33320	-11.33310
		-8.32602	-8.32484		-10.54250	-10.53600		-12.54680	-12.54560
		-8.75228	-8.75438		-11.39990	-11.39620		-13.78530	-13.7842
		-9.18778	-9.18753		-12.27470	-12.27480		-15.04390	-15.03500

Table 4
 The values of $H'''(1)$

R	γ	HPM	FDM	γ	HPM	FDM	γ	HPM	FDM
1	0.1	-5.80025	-5.80306	0.2	-5.63807	-5.63422	0.3	-5.50384	-5.50611
		-5.05615	-5.05086		-4.36864	-4.37014		-3.85088	-3.84827
		-4.24116	-4.24125		-3.13242	-3.13691		-2.40081	-2.40746
		-3.54137	-3.54191		-2.21298	-2.21168		-1.45639	-1.45615
		-2.94383	-2.94079		-1.54154	-1.5471		-0.86164	-0.86394
		-2.43643	-2.43943		-1.05973	-1.05512		-0.49849	-0.49892
		-2.00791	-2.00790		-0.71965	-0.71788		-0.28276	-0.28546
		-1.64795	-1.64880		-0.48327	-0.48724		-0.15690	-0.15913
		-1.34714	-1.34524		-0.32124	-0.32270		-0.07271	-0.08410

Table 5
 The values of $f'(0)$

R	γ	HPM	FDM	γ	HPM	FDM	γ	HPM	FDM
1	0.1	-1.02714	-1.0405	0.2	-1.04956	-1.07363	0.3	-1.06840	-1.10122
5		-1.13317	-1.19472		-1.23951	-1.34366		-1.32640	-1.46170
10		-1.26030	-1.37214		-1.45998	-1.63757		-1.61826	-1.8389
15		-1.38184	-1.53543		-1.66400	-1.89593		-1.88179	-2.16140
20		-1.49823	-1.68688		-1.85374	-2.12758		-2.12196	-2.44594
25		-1.60986	-1.82839		-2.03106	-2.33904		-2.34277	-2.70287
30		-1.71708	-1.96143		-2.19755	-2.53408		-2.54739	-2.93858
35		-1.82022	-2.08728		-2.35453	-2.71633		-2.73840	-3.15756
40		-1.91957	-2.20666		-2.50318	-2.88785		-2.91773	-3.36269

Table 6
 The values of $f'(1)$

R	γ	HPM	FDM	γ	HPM	FDM	γ	HPM	FDM
1	0.1	-0.95984	-0.95126	0.2	-0.92751	-0.91248	0.3	-0.90093	-0.88092
5		-0.81349	-0.77913		-0.68298	-0.63303		-0.58787	-0.53103
10		-0.65931	-0.60729		-0.46073	-0.40076		-0.33760	-0.28156
15		-0.53239	-0.47331		-0.30712	-0.25316		-0.18967	-0.14839
20		-0.42835	-0.36872		-0.20243	-0.15940		-0.10447	-0.07759
25		-0.34344	-0.28757		-0.13203	-0.09994		-0.05654	-0.04022
30		-0.27441	-0.22324		-0.08529	-0.06239		-0.03013	-0.02068
35		-0.21854	-0.17342		-0.05462	-0.03877		-0.01573	-0.01055
40		-0.17350	-0.134573		-0.03470	-0.02398		-0.00615	-0.00534

5. Conclusions

A careful analyses of literature review and our results makes us to conclude, Casson fluid enhance the efficiency of porous slider bearing. The values representing for $H''(0), H'''(0), f'(0)$ with fixed value of Casson parameter γ are increasing in magnitude as Reynolds number increases. But in case of $H''(1), H'''(1), f'(1)$ for fixed value of γ absolute values are decreasing in magnitude with increasing in Reynolds numbers. It is observed that this is due to the injection effect at $\eta = 1$. Further friction between two plates is greatly reduced due to lubrication of Casson fluid. Due to this, the application of such models is used in the growth of industry and technology.

Acknowledgement

This research was not funded by any grant. The authors thank the referees for their valuable suggestions in the revising the research paper.

References

- [1] Berman, Abraham S. "Laminar flow in channels with porous walls." *Journal of Applied physics* 24, no. 9 (1953): 1232-1235.
<https://doi.org/10.1063/1.1722307>
- [2] Elkouh, A. F. "Laminar source flow between parallel porous disks." *Applied Scientific Research* 21, no. 1 (1969): 284-302.
<https://doi.org/10.1007/B F00411613>
- [3] Terrill, R. M., and P. W. Thomas. "On laminar flow through a uniformly porous pipe." *Applied Scientific Research* 21, no. 1 (1969): 37-67.
<https://doi.org/10.1007/B F00411613>
- [4] Wang, Chang-Yi. "Symmetric viscous flow between two rotating porous discs—moderate rotation." *Quarterly of Applied Mathematics* 34, no. 1 (1976): 29-38.
<https://doi.org/10.1090/qam/99656>

- [5] Gorla, Rama Subba Reddy. "Flow and thermal characteristics of a circular porous slider bearing." *Wear* 94, no. 2 (1984): 157-174.
[https://doi.org/10.1016/0043-1648\(84\)90052-8](https://doi.org/10.1016/0043-1648(84)90052-8)
- [6] Bujurke, N. M., H. P. Patil, and S. G. Bhavi. "Porous slider bearing with couple stress fluid." *Acta mechanica* 85, no. 1-2 (1990): 99-113.
<https://doi.org/10.1007/BF01213545>
- [7] Singh, Jay Pal, and Naseem Ahmad. "Analysis of a porous-inclined slider bearing lubricated with magnetic fluid considering thermal effects with slip velocity." *Journal of the Brazilian Society of Mechanical Sciences and Engineering* 33, no. 3 (2011): 351-356.
<https://doi.org/10.1590/S1678-58782011000300011>
- [8] Singh, Udaya P., and R. S. Gupta. "Dynamic performance characteristics of a curved slider bearing operating with ferrofluids." *Advances in Tribology* 2012 (2012): 1-6.
<https://doi.org/10.1155/2012/278723>
- [9] He, Ji-Huan. "Recent development of the homotopy perturbation method." *Topological methods in nonlinear analysis* 31, no. 2 (2008): 205-209.
- [10] Gupta, Sumit, Devendra Kumar, and Jagdev Singh. "Application of He's homotopy perturbation method for solving nonlinear wave-like equations with variable coefficients." *International Journal of Advances in Applied Mathematics and Mechanics* 1, no. 2 (2013): 65-79.
- [11] Abbasbandy, S. "Application of He's homotopy perturbation method to functional integral equations." *Chaos, Solitons & Fractals* 31, no. 5 (2007): 1243-1247.
<https://doi.org/10.1016/j.chaos.2005.10.069>
- [12] Ganji, D. D., and A. Sadighi. "Application of He's homotopy-perturbation method to nonlinear coupled systems of reaction-diffusion equations." *International Journal of Nonlinear Sciences and Numerical Simulation* 7, no. 4 (2006): 411-418.
<https://doi.org/10.1515/IJNSNS.2006.7.4.411>
- [13] Rafei, M., and D. D. Ganji. "Explicit solutions of Helmholtz equation and fifth-order KdV equation using homotopy perturbation method." *International Journal of Nonlinear Sciences and Numerical Simulation* 7, no. 3 (2006): 321-328.
<https://doi.org/10.1515/IJNSNS.2006.7.3.321>
- [14] Rafei, M., D. D. Ganji, and H. Daniali. "Solution of the epidemic model by homotopy perturbation method." *Applied Mathematics and Computation* 187, no. 2 (2007): 1056-1062.
<https://doi.org/10.1016/j.amc.2006.09.019>
- [15] Kumar, VS Sampath, and N. P. Pai. "Analysis of porous elliptical slider through semi-analytical technique." *Journal of Advanced Research in Fluid Mechanics and Thermal Sciences* 48, no. 1 (2018): 80-90.
- [16] VS, Sampath Kumar, and Nithyananda P. Pai. "Suction and Injection Effect on Flow Between Two Plates with Reference to Casson Fluid Model." *Multidiscipline Modeling in Materials and Structures* 15, no.3 (2018): 558-574.
<https://doi.org/10.1108/MMMS-05-2018-0092>
- [17] K umar, V. S., and N. Pai. "A Study of Magnetic Effect on Flow Between Two Plates with Suction or Injection with Special Reference to Casson fluid." *Frontiers in Heat and Mass Transfer* 13, no. 23 (2019): 1-9.
<http://dx.doi.org/10.5098/hmt.12.23>
- [18] Siddiqui, Abdul M., Sania Irum, and Ali R. Ansari. "Unsteady squeezing flow of a viscous MHD fluid between parallel plates, a solution using the homotopy perturbation method." *Mathematical Modelling and Analysis* 13, no. 4 (2008): 565-576.
<https://doi.org/10.3846/1392-6292.2008.13.565-576>
- [19] Babolian, Esmail, A. Azizi, and J. Saeidian. "Some notes on using the homotopy perturbation method for solving time-dependent differential equations." *Mathematical and computer modelling* 50, no. 1-2 (2009): 213-224.
<https://doi.org/10.1016/j.mcm.2009.03.003>
- [20] Shaw, Sachin, Ganeswar Mahanta, and Mrutyunjay Das. "Thermal and solutal Marangoni stagnation point Casson fluid flow over a stretching sheet in the presence of radiation, Soret and Dofour effect with chemical reaction." *Heat Transfer—Asian Research* 48, no. 1 (2019): 323-342.
<https://doi.org/10.1002/htj.21386>
- [21] Shaw, Sachin, A. S. Dogonchi, M. K. Nayak, and O. D. Makinde. "Impact of Entropy Generation and Nonlinear Thermal Radiation on Darcy–Forchheimer Flow of MnFe₂O₄-Casson/Water Nanofluid due to a Rotating Disk: Application to Brain Dynamics." *Arabian Journal for Science and Engineering* (2020): 1-20.
<https://doi.org/10.1007/s13369-020-04453-2>